Spin Hall effect of a light beam in left-handed materials

Hailu Luo, Shuangchun Wen,* Weixing Shu, Zhixiang Tang, Yanhong Zou, and Dianyuan Fan
Key Laboratory for Micro/Nano Opto-Electronic Devices of Ministry of Education, School of Computer and Communication, Hunan University, Changsha 410082, China
(Received 8 June 2009; published 12 October 2009)

We establish a general propagation model to describe the spin Hall effect of light beam in left-handed materials (LHMs). A spin-dependent shift of the beam centroid perpendicular to the refractive index gradient for the light beam through an air-LHM interface is demonstrated. For a certain circularly polarized component, whether the transverse shift is positive or negative depends on the magnitude of the refractive index gradient. Very surprisingly, the spin Hall effect in the LHM is unreversed, although the sign of refractive index gradient is reversed. The physics underlying this counterintuitive effect is that the spin angular momentum of photons is unreversed. Further, we reveal that the angular shift in the LHM is reversed due to the negative diffraction. These findings provide alternative evidence for that the linear momentum of photons is reversed, while the spin angular momentum is unreversed in the LHM.

DOI: 10.1103/PhysRevA.80.043810 PACS number(s): 42.25.−p, 42.79.−e, 41.20.Jb, 78.20.Ci

I. INTRODUCTION

The spin Hall effect of light is the photonic version of the spin Hall effect in electronic systems [1–3], in which the spin photons play the role of the spin charges, and a refractive index gradient plays the role of the electric potential gradient [4,5]. Such a spatial gradient for the refractive index could occur at an interface between two materials. The spin Hall effect manifests itself as a spin-dependent shift of the beam centroid perpendicular to the refractive index gradient when photons passing through the interface. For left and right circularly polarized beams, the eigenvalues of the transverse shift are the same in magnitude but opposite in direction. In fact, the translational inertial spin effect has been predicted by Beauregard more than 40 years ago [6]. This effect is significantly different from longitudinal Goos-Hänchen shift [7] and transverse Imbert-Fedorov shift [8,9] in total internal reflection, which are described as evanescent-wave penetration. The splitting in the spin Hall effect, implied by angular-momentum conservation, takes place as a result of an effective spin-orbit interaction. In a glass-air interface, the spin-dependent transverse shifts are just a few tens of nanometers. This is the reason why the tiny scale of the effect escaped detection for a long time. More recently, the spin Hall effect has been detected in experiment via quantum weak measurements [10].

The recent advent of negative-refraction materials [11], also known as left-handed materials (LHMs) [12], not only opens a new way to generate the magnitude of refractive index gradient, but also provides an unprecedented reverse of the sign of refractive index at the interface of an ordinary right-handed material (RHM) and a LHM. It is now conceivable that LHMs can be constructed whose permittivity and permeability values may be designed to vary independently and arbitrarily, taking negative or near-zero value as desired [13]. Hence, it is possible for designing a certain refractive index gradient to modulate the spin Hall effect. The potential interests encourage us to explore what would happen to the spin Hall effect of light beam in the air-LHM interface. In the past several years, many counterintuitive phenomena, such as anomalous evanescent-wave amplification [14], unusual photon tunneling [15], negative Goos-Hänchen shift [16], reversed Doppler effect [17], and inverted Cherenkov effect [18] in LHMs have been reported. Now a question naturally arise. Is the spin Hall effect reversed as expected? In addition, due to the different arguments on the direction of linear momentum in LHMs [19–22], the issue of how to describe photon momentum is still an open problem. Hence, another motivation is to clarify whether the photon momentum is reversed in the LHM. In principle, the reflection and transmission from the air-LHM interface should fulfill the total momentum conservation law. We believe that the study of the spin Hall effect may provide insights into the fundamental properties of photon momentum in the LHMs.

In this work, we use an air-LHM interface as the refractive index gradient to explore what would happen to the spin Hall effect of light beam. First, starting from the representation of a plane-wave angular spectrum, we establish a general beam propagation model to describe the beam reflection and transmission. Next, we uncover how the beam evolves and how the spin Hall effect affects its transverse shifts. It is necessary to consider the spin Hall effect in the presence of loss, since the loss is inherent to realizable LHMs. For the purpose of comparison, we also study the spin Hall effect in the air-RHM interface. Then, we examine what roles the magnitude and the sign of the refractive index gradient play in the spin Hall effect. Finally, we explore whether the spin-dependent transverse shift or diffraction-dependent angular shift is reversed. The transverse shifts and the angular shifts, governed by the total momentum conservation law, provide us a new way to clarify the nature of photon momentum in the LHMs.

II. BEAM REFLECTION AND TRANSMISSION

We begin to establish a general beam propagation model for describing light beam reflection and refraction from a

*scwen@hnu.cn

 ©2009 The American Physical Society

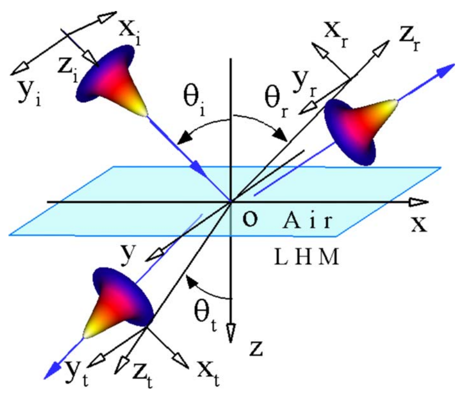

FIG. 1. (Color online) Geometry of the beam reflection and transmission from an air-LHM interface. The reflected and transmitted beams will undergo the longitudinal shift, the transverse shift, and the angular shift.

planar air-LHM interface. Figure 1 illustrates the Cartesian coordinate system. The z axis of the laboratory Cartesian frame (x,y,z) is normal to the air-LHM interface located at $z=0$. We use the coordinate frames (x_a,y_a,z_a) for individual beams, where $a=i,r,t$ denotes incident, reflected, and transmitted beams, respectively. In the paraxial optics, the incident field of an arbitrarily polarized beam can be written as

$$\mathbf{E}_i(x_i,y_i,z_i) \propto (\alpha\mathbf{e}_{ix}+\beta\mathbf{e}_{iy})\exp\left[-\frac{k_0}{2}\frac{x_i^2+y_i^2}{z_R+iz_i}\right]. \tag{1}$$

Here, $z_R=k_0w_0^2/2$ is the Rayleigh length and $k_0=\omega/c$ is the wave number in the air. The coefficients α and β satisfy the relation $\sigma=i(\alpha\beta^*-\alpha^*\beta)$. The polarization operator $\sigma=\pm1$ corresponds to left- and right-handed circularly polarized lights, respectively. It is well known that circularly polarized Gaussian beam can carry spin angular momentum $\sigma\hbar$ per photon due to its polarization state [23].

We first explore the reflected field, which can be solved by employing the Fourier transformations. The complex amplitude can be conveniently expressed as

$$\mathbf{E}_r(x_r,y_r,z_r) = \int dk_{rx}dk_{ry}\tilde{\mathbf{E}}_r(k_{rx},k_{ry}) \times\exp[i(k_{rx}x_r+k_{ry}y_r+k_{rz}z_r)], \tag{2}$$

where $k_{rz}=\sqrt{k_0^2-(k_{rx}^2+k_{ry}^2)}$. From a mathematical point of view, the approximate paraxial expression for the field in Eq. (2) can be obtained by the expansion of the square root of k_{rz} to the first order [24], which yields

$$\mathbf{E}_r = \exp(ik_0z)\int dk_{rx}dk_{ry}\tilde{\mathbf{E}}_r(k_{rx},k_{ry}) \times\exp\left[i\left(k_{rx}x_r+k_{ry}y_r-\frac{k_{rx}^2+k_{ry}^2}{2k_0}z\right)\right]. \tag{3}$$

The reflected angular spectrum $\tilde{E}_r(k_{rx},k_{ry})$ is related to the boundary distribution of the electric field by means of the relation [5]

$$\tilde{\mathbf{E}}_r = \begin{bmatrix} r_p & \dfrac{k_{ry}\cot\theta_i}{k_0}(r_p+r_s) \\ -\dfrac{k_{ry}\cot\theta_i}{k_0}(r_p+r_s) & r_s \end{bmatrix}\tilde{\mathbf{E}}^r_{p,s}, \tag{4}$$

where r_p and r_s are the Fresnel reflection coefficients. From the Snell's law, we can get $k_{rx}=-k_{ix}$ and $k_{ry}=k_{iy}$. Combining with boundary condition, we get

$$\tilde{\mathbf{E}}^r_{p,s} \propto (\alpha\mathbf{e}_{rx}+\beta\mathbf{e}_{ry})\exp\left[-\frac{z_R(k_{rx}^2+k_{ry}^2)}{2k_0}\right]. \tag{5}$$

In fact, after the electric field on the plane $z_r=0$ is known, Eq. (3) together with Eqs. (4) and (5) provides the expression of the field in the space $z_r>0$,

$$\begin{aligned}\mathbf{E}_r \propto {} & \left[\alpha r_p\left(1-i\frac{x_r}{z_R+iz_r}\frac{\partial\ln r_p}{\partial\theta_i}\right)+i\beta\frac{y_r}{z_R+iz_r}\right.\\ & \left.\times(r_p+r_s)\cot\theta_i\right]\exp\left[-\frac{k_0}{2}\frac{x_r^2+y_r^2}{z_R+iz_r}\right]\mathbf{e}_{rx}\\ & +\left[\beta r_s\left(1-i\frac{x_r}{z_R+iz_r}\frac{\partial\ln r_s}{\partial\theta_i}\right)-i\alpha\frac{y_r}{z_R+iz_r}\right.\\ & \left.\times(r_p+r_s)\cot\theta_i\right]\exp\left[-\frac{k_0}{2}\frac{x_r^2+y_r^2}{z_R+iz_r}\right]\mathbf{e}_{ry}.\end{aligned} \tag{6}$$

Note that the above expression of reflected field coincides with the early results [25–27] for the reflection in air-RHM interface, while the reflection coefficients are significantly different at the air-LHM interface. Hence, the spatial profile of the reflected beam is also evidently altered.

We next explore the transmitted field. Similarly, the complex amplitude in the LHM can be written as

$$\mathbf{E}_t(x_t,y_t,z_t) = \int dk_{tx}dk_{ty}\tilde{\mathbf{E}}_t(k_{tx},k_{ty})\exp[i(k_{tx}x_t+k_{ty}y_t)+ik_{tz}z_t], \tag{7}$$

where $k_{tz}=-\sqrt{n^2k_0^2-(k_{tx}^2+k_{ty}^2)}$ and n is the refractive index of the LHM. The choice of negative sign of k_{tz} ensures that power propagates away from the surface to the $+z$ direction [12]. In the paraxial approximation, we have

$$\mathbf{E}_t = \exp(ink_0z)\int dk_{tx}dk_{ty}\tilde{\mathbf{E}}_t(k_{tx},k_{ty}) \times\exp\left[i\left(k_{tx}x_t+k_{ty}y_t-\frac{k_{tx}^2+k_{ty}^2}{2nk_0}z\right)\right]. \tag{8}$$

We note that the field of paraxial beams in LHMs can be written in the similar way to that in RHMs, while wave vector components undergo the negative refraction.

The transmitted angular spectrum $\tilde{E}_t(k_{tx},k_{ty})$ in Eq. (8) is related to the boundary distribution of the electric field by means of the relation

$$\tilde{\mathbf{E}}_t = \begin{bmatrix} t_p & \dfrac{k_{ty}\cot\theta_i}{k_0}(t_p - \eta t_s) \\ \dfrac{k_{ty}\cot\theta_i}{k_0}(\eta t_p - t_s) & t_s \end{bmatrix} \tilde{\mathbf{E}}^t_{p,s}, \quad (9)$$

where $\eta = \cos\theta_t/\cos\theta_i$ and t_p and t_s are the Fresnel transmission coefficients. From the Snell's law under the paraxial approximation, $k_{tx} = k_{ix}/\eta$ and $k_{ty} = k_{iy}$, we obtain

$$\tilde{\mathbf{E}}^t_{p,s} \propto (\alpha \mathbf{e}_{tx} + \beta \mathbf{e}_{ty}) \exp\left[-\frac{z_{Rx}k_{tx}^2 + z_{Ry}k_{ty}^2}{2nk_0} \right]. \quad (10)$$

The interesting point we want to stress is that there are two different Rayleigh lengths, $z_{Rx} = n\eta^2 k_0 w_0^2/2$ and $z_{Ry} = nk_0 w_0^2/2$, characterizing the spreading of the beam in the direction of x and y axes, respectively [28]. Substituting Eqs. (9) and (10) into Eq. (8), we obtain the transmitted field in the space $z_t > 0$,

$$\begin{aligned} \mathbf{E}_t \propto & \exp\left[-\frac{nk_0}{2}\left(\frac{x_t^2}{z_{Rx}+iz_t} + \frac{y_t^2}{z_{Ry}+iz_t} \right) \right] \\ & \times \left[\alpha t_p \left(1 + i\frac{n\eta x_t}{z_{Rx}+iz_t}\frac{\partial \ln t_p}{\partial \theta_i} \right) + i\beta \frac{ny_t}{z_{Ry}+iz_t} \right. \\ & \left. \times (t_p - \eta t_s)\cot\theta_i \right] \mathbf{e}_{tx} \\ & + \exp\left[-\frac{nk_0}{2}\left(\frac{x_t^2}{z_{Rx}+iz_t} + \frac{y_t^2}{z_{Ry}+iz_t} \right) \right] \\ & \times \left[\beta t_s \left(1 + i\frac{n\eta x_t}{z_{Rx}+iz_t}\frac{\partial \ln t_s}{\partial \theta_i} \right) \right. \\ & \left. + i\alpha \frac{ny_t}{z_{Ry}+iz_t}(\eta t_p - t_s)\cot\theta_i \right] \mathbf{e}_{ty}. \end{aligned} \quad (11)$$

A further important point should be noted is that we have introduced negative Rayleigh length or negative diffraction. The inherent physics underlying the negative diffraction is the angular spectrum components undergo a negative phase velocity [29].

III. SPIN HALL EFFECT

In order to accurately describe the spin Hall effect, the issue of loss of the LHM should be involved. Hence, a certain dispersion relation, such as the Lorentz medium model, should be introduced. The constitutive parameters are

$$\varepsilon(\omega) = 1 - \frac{\omega_{ep}^2}{\omega^2 - \omega_{eo}^2 + i\omega\gamma_e}, \quad (12)$$

$$\mu(\omega) = 1 - \frac{F\omega_{mp}^2}{\omega^2 - \omega_{mo}^2 + i\omega\gamma_m}. \quad (13)$$

To avoid the trouble involving a certain value of frequency, we assume the material parameters are $\omega_{eo} = \omega_{mo} = \omega_o$, $\omega_{ep} = \omega_{mp} = \omega_o$, $F = 1.52$, and $\gamma_e = \gamma_m = 0.001\omega_0$. Note that the Goos-Hänchen longitudinal shift and Imbert-Fedorov transverse shift in such a metamaterial have received much attentions [16,30]. Here we want to explore what would happen to the spin Hall effect of light beam.

The intensity distribution of electromagnetic fields is closely linked to the Poynting vector [31] $I(x_a, y_a, z_a) \propto \mathbf{S}_a \cdot \mathbf{e}_{az}$. Here, the Poynting vector is given by $\mathbf{S}_a \propto \mathrm{Re}[\mathbf{E}_a^* \times \mathbf{H}_a]$ and the magnetic field can be obtained by $\mathbf{H}_a = -i\mu^{-1}\nabla \times \mathbf{E}_a$. At any given plane $z_a = \text{const}$, the beam centroid is given by [26] $\langle \mathbf{m}_a \rangle = \langle x_a \rangle \mathbf{e}_{ax} + \langle y_a \rangle \mathbf{e}_{ay}$, where

$$\langle \mathbf{m}_a \rangle = \frac{\int\int \mathbf{m}_a I(x_a, y_a, z_a) dx_a dy_a}{\int\int I(x_a, y_a, z_a) dx_a dy_a}. \quad (14)$$

Because of the spin Hall effect, a linear polarized Gaussian beam will be divided into two circularly polarized components with opposite shifts.

To illustrate the shifts, we now determine the centroid of the reflected beam. Substituting Eq. (6) into Eq. (14), we can obtain the longitudinal and the transverse shifts. The longitudinal shift can be written as a sum of two terms $D_x^r = \Delta x_r + \delta x_r$, and

$$\Delta x_r = \frac{1}{k_0}\frac{\xi_p |r_p|^2 f_p^2 + \xi_s |r_s|^2 f_s^2}{|r_p|^2 f_p^2 + |r_s|^2 f_s^2}, \quad (15)$$

$$\delta x_r = -\frac{z_r}{k_0 z_R}\frac{\rho_p |r_p|^2 f_p^2 + \rho_s |r_s|^2 f_s^2}{|r_p|^2 f_p^2 + |r_s|^2 f_s^2}. \quad (16)$$

In a similar way, the transverse shift can also be divided into two terms $D_y^r = \Delta y_r + \delta y_r$, we find

$$\begin{aligned} \Delta y_r = & -\frac{1}{k_0}\frac{f_p f_s \cot\theta_i}{|r_p|^2 f_p^2 + |r_s|^2 f_s^2}[(|r_p|^2 + |r_s|^2)\sin\psi \\ & + 2|r_p||r_s|\sin(\psi - \phi_p + \phi_s)], \end{aligned} \quad (17)$$

$$\delta y_r = \frac{z_r}{k_0 z_R}\frac{f_p f_s (|r_p|^2 - |r_s|^2)\cot\theta_i \cos\psi}{|r_p|^2 f_p^2 + |r_s|^2 f_s^2}. \quad (18)$$

Here, $r_A = |r_A|\exp(i\phi_A)$, $A \in \{p, s\}$, $\alpha = f_p \in \mathbf{R}$, $\beta = f_s \exp(i\psi)$, $\rho_A = \mathrm{Re}[\partial \ln r_A / \partial\theta_i]$, and $\xi_A = \mathrm{Im}[\partial \ln r_A/\partial\theta_i]$. From Eqs. (15)–(18), we can find that both the longitudinal shift and the transverse shift can be written as a combination of z_r-independent term and z_r-dependent term. Note that the z_r-independent term longitudinal shifts are reversed in the air-LHM interface, which coincides well with the early prediction [16].

The z_r-dependent term can be regarded as a small angler shift inclining from the axis of beam centroid. The corresponding longitudinal and transverse divergence angles are given by $\delta x_r = z_r \Delta\theta_{rx}$ and $\delta y_r = z_r \Delta\theta_{ry}$, such that

$$\Delta\theta_{rx} = -\frac{1}{k_0 z_R}\frac{\rho_p |r_p|^2 f_p^2 + \rho_s |r_s|^2 f_s^2}{|r_p|^2 f_p^2 + |r_s|^2 f_s^2}, \quad (19)$$

$$\Delta\theta_{ry} = \frac{1}{k_0 z_R}\frac{f_p f_s (|r_p|^2 - |r_s|^2)\cot\theta_i \cos\psi}{|r_p|^2 f_p^2 + |r_s|^2 f_s^2}. \quad (20)$$

Here, the longitudinal divergence angle is polarization independent, while the transverse divergence angle depends on

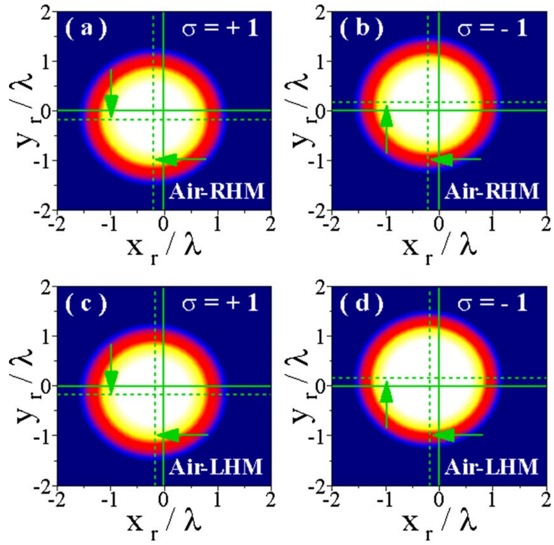

FIG. 2. (Color online) The spin Hall effect induces transverse shifts for the reflected beam at the interface between air and low-refractive index medium. [(a) and (b)] Intensity distributions of the $\sigma=+1$ and $\sigma=-1$ beams reflected from the air-RHM interface. [(c) and (d)] Intensity distributions of the $\sigma=+1$ and $\sigma=-1$ beams reflected from air-LHM interface. The incident angle of the beam is chosen as $\theta_i=\pi/6$. The material parameters of LHM are $\omega=1.414\omega_0$, $\varepsilon=-1+0.003i$, and $\mu=-0.52+0.002i$. To generate a reversed sign of refractive index gradient, the material parameters of RHM are chosen as $\varepsilon=1+0.003i$ and $\mu=0.52+0.002i$. The intensity distributions in the plane $z_r=z_R$ are plotted in normalized units.

the polarization. For a linear or a circularly beam, the condition $\cos\psi=0$ is satisfied and the transverse divergence angle vanishes.

To illustrate the spin Hall effect, we consider a light beam incident from air to a low-refractive-index medium. Here, the low-refractive-index medium means that the values of the indices of the RHM and the LHM are less than the index of air. In the case of reflection from the air-RHM interface, the left circularly polarized beam undergoes a negative transverse shift, while the right circularly polarized beam exhibits a positive transverse shift [Figs. 2(a) and 2(b)]. Compare to the transverse shifts in the air-RHM interface, we easily find that the corresponding shifts in the air-LHM interface is unreversed [Figs. 2(c) and 2(d)]. The unreversed transverse shifts mean that the spin Hall effect in the reflected beam is also unreversed. In the absence of loss, the longitudinal shifts should vanish since the Fresnel coefficients are real [32]. In our case, however, the longitudinal shifts present due to the loss inherent in the LHM. Note that the longitudinal shifts in Fig. 2 is unreversed in the LHM because the unreversed angular shift eliminate the reversed z_r-independent shift.

We now discuss the beam centroid of the transmitted beam. After substituting Eq. (11) into Eq. (14), we can obtain the longitudinal shift and the transverse shift. The longitudinal shift can be written as a sum of two terms $D_x^t=\Delta x_t+\delta x_t$, then

$$\Delta x_t=-\frac{\eta}{k_0}\frac{\zeta_p|t_p|^2f_p^2+\zeta_s|t_s|^2f_s^2}{|t_p|^2f_p^2+|t_s|^2f_s^2}, \tag{21}$$

$$\delta x_t=\frac{\eta z_t}{k_0 z_{Rx}}\frac{\varrho_p|t_p|^2f_p^2+\varrho_s|t_s|^2f_s^2}{|t_p|^2f_p^2+|t_s|^2f_s^2}. \tag{22}$$

In an analogous manner, the transverse shift can also be separated into two terms $D_y^t=\Delta y_t+\delta y_t$, and

$$\Delta y_t=-\frac{1}{k_0}\frac{f_pf_s\cot\theta_i}{|t_p|^2f_p^2+|t_s|^2f_s^2}[(|t_p|^2+|t_s|^2)\sin\psi + 2\eta|t_p||t_s|\sin(\psi-\varphi_p+\varphi_s)], \tag{23}$$

$$\delta y_t=\frac{z_t}{k_0 z_{Ry}}\frac{f_pf_s(|t_p|^2-|t_s|^2)\cot\theta_i\cos\psi}{|t_p|^2f_p^2+|t_s|^2f_s^2}. \tag{24}$$

Here, $t_A=|t_A|\exp(i\varphi_A)$, $\varrho_A=\mathrm{Re}[\partial\ln t_A/\partial\theta_i]$, and $\zeta_A=\mathrm{Im}[\partial\ln t_A/\partial\theta_i]$. It should be mentioned that δx_t and δy_t are given by functions of Rayleigh lengths z_{Rx} and z_{Ry}, respectively. Hence, the angular shifts are purely diffraction effect.

For the transmitted beam, the longitudinal and the transverse divergence angles are given by $\delta x_t=z_t\Delta\theta_{tx}$ and $\delta y_t=z_t\Delta\theta_{ty}$, we have

$$\Delta\theta_{tx}=\frac{\eta}{k_0 z_{Rx}}\frac{\varrho_p|t_p|^2f_p^2+\varrho_s|t_s|^2f_s^2}{|t_p|^2f_p^2+|t_s|^2f_s^2}, \tag{25}$$

$$\Delta\theta_{ty}=\frac{1}{k_0 z_{Ry}}\frac{f_pf_s(|t_p|^2-|t_s|^2)\cot\theta_i\cos\psi}{|t_p|^2f_p^2+|t_s|^2f_s^2}. \tag{26}$$

In principle, reflection and refraction of waves at the interface between two homogeneous media are described by the Snell's law. However, the angular divergences mean that the Snell's law cannot accurately describe such phenomena [33]. Thus, the Snell's law needs to be extended to include spinning photons.

In the spin Hall effect of light, the refractive index gradient plays the role of the electric potential gradient. Hence we attempt to examine what roles the magnitude and the sign of the refractive index gradient play in the spin Hall effect. We first consider the beam incident from air to a low-refractive-index medium. For the left circularly polarized component $\sigma=+1$, the transmitted field exhibits a negative transverse shift [Figs. 3(a) and 3(c)]. The right circularly polarized component $\sigma=-1$ also presents a transverse shift, but in the opposite direction [Figs. 3(b) and 3(d)]. Very surprisingly, the transverse shift caused by the spin Hall effect in the LHM is unreversed, although the sign of refractive index gradient is reversed. These results have also been proved by Krowne in his interesting work [34]. Furthermore, we want to explore whether a reversed magnitude of refractive index gradient can lead to a reversed spin Hall effect.

To generate a reversed magnitude of refractive index gradient, we next investigate the beam incident from air to a high-refractive-index medium. Here, the high-refractive-index medium means the values of the indices of the RHM and the LHM are larger than the index of air. For the left circularly polarized component $\sigma=+1$, the transmitted field exhibits a positive transverse shift [Figs. 4(a) and 4(c)]. For the right circularly polarized component $\sigma=-1$, however, the transmitted field presents a negative transverse shift [Figs. 4(b) and 4(d)]. We can find that the transverse shifts in the

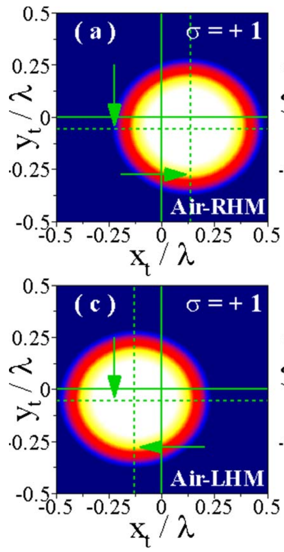

FIG. 3. (Color online) The spin Hall effect induces transverse shifts for the transmitted beam from air to low-refractive-index medium. [(a) and (b)] Intensity distributions of the transmission beam in the RHM for $\sigma=+1$ and $\sigma=-1$ components, respectively. [(c) and (d)] Intensity distributions of the transmitted beam in the LHM for $\sigma=+1$ and $\sigma=-1$ components, respectively. The incident angle of the beam is chosen as $\theta_i=\pi/6$. The material parameters are the same as in Fig. 2. The intensity distributions in the plane $z_t=z_R$ are plotted in normalized units.

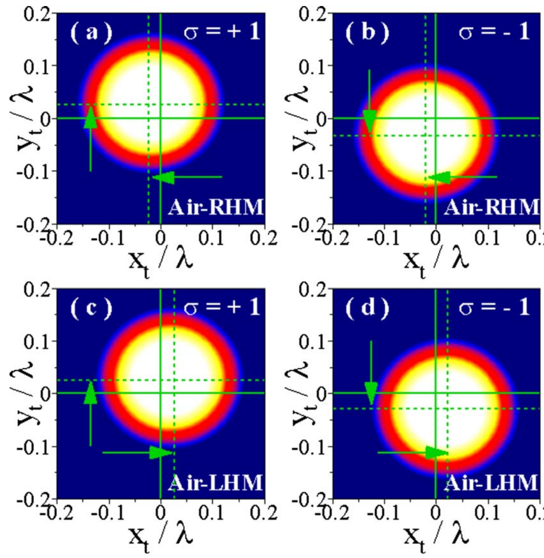

FIG. 4. (Color online) The spin Hall effect induces transverse shifts for the transmitted beam from air to high-refractive-index medium. [(a) and (b)] Intensity distributions of the transmitted beam in the RHM for $\sigma=+1$ and $\sigma=-1$ components, respectively. [(c) and (d)] Intensity distributions of the transmitted beam in the LHM for $\sigma=+1$ and $\sigma=-1$ components, respectively. The incident angle of the beam is chosen as $\theta_i=\pi/6$. To generate a high-refractive index, the material parameters of LHM are $\varepsilon=-2+0.003i$ and $\mu=-1.52+0.002i$. For comparison, the material parameters of RHM are chosen as $\varepsilon=2+0.003i$ and $\mu=1.52+0.002i$. The intensity distributions in the plane $z_t=z_R$ are plotted in normalized units.

LHM are unreversed, while the angular shifts are reversed because of the negative diffraction. Comparing Fig. 3 to Fig. 4 shows that whether the spin Hall effect is reversed depends on the magnitude the refractive index gradient but independent on its sign.

In order to reveal the physics underlying the unreversed spin Hall effect, we focus on the momentum conservation laws which govern the beam reflection and transmission. The monochromatic beam can be formulated as a localized wave packet whose spectrum arbitrarily narrows [25]. Let ath packet include N_a photons, i.e., its field energy is $W_a=N_a\omega$. The linear momentum of the ath packet is $\mathbf{p}_a=N_a\mathbf{k}_c^a$ (we set $\hbar=c=1$) and the conservation law for the linear momentum can be written as $p^i_{x,y}=p^r_{x,y}+p^t_{x,y}$. For the x component, we have $p^i_x=N_ik_i\sin\theta_i$, $p^r_x=N_rk_r\sin\theta_r+N_rk_r\Delta\theta_{rx}\cos\theta_r$, and $p^t_x=N_tk_t\sin\theta_t+N_tk_t\Delta\theta_{tx}\cos\theta_t$. For the y component, we get $p^i_y=0$, $p^r_y=N_rk_r\Delta\theta_{rx}$, and $p^t_y=N_tk_t\Delta\theta_{tx}$. In the absence of loss, the total number of photons remain unchanged $N_r+N_t=N_i$. The angular shifts should fulfill conservation law for x and y components of the linear momentum

$$-Q_r\Delta\theta_{rx}\cos\theta_r+nQ_t\Delta\theta_{tx}\cos\theta_t=0, \tag{27}$$

$$-Q_r\Delta\theta_{rx}+nQ_t\Delta\theta_{ty}=0. \tag{28}$$

Here, $Q_r=N_r/N_i$ and $Q_t=N_t/N_i$ are the energy reflection and transmission coefficients, respectively. In the frame of classic electrodynamics, $Q_r=f_p^2|r_p|^2+f_s^2|r_s|^2$ and $Q_t=n\eta(f_p^2|t_p|^2+f_s^2|t_s|^2)/\mu$, the conservation law, Eqs. (27) and (28), still holds true. These results coincide well with the linear momentum conservation laws in RHMs [32,35], although the sign of refractive index is reversed. From the linear momentum conservation law, we find that the reversed divergence angles mean the linear momentum of photons should be reversed.

We proceed to consider the total angular-momentum conservation law. The z component of total angular momentum of per one photon can be represented as a sum of the extrinsic orbital angular momentum and intrinsic spin angular momentum [25]

$$j_{rz}=-\Delta y_rk_r\sin\theta_r+\sigma_r\cos\theta_r, \tag{29}$$

$$j_{tz}=-\Delta y_tk_t\sin\theta_t+\sigma_t\cos\theta_t. \tag{30}$$

The transverse shifts of the wave packet fulfill the conservation law for the total angular momentum [36,37]

$$Q_r(S_{rz}-\Delta y_rk_r\sin\theta_r)+Q_t(S_{tz}-\Delta y_tk_t\sin\theta_t)=S_{iz}. \tag{31}$$

The z components of the spin angular momenta are given by $S_{iz}=\sigma\cos\theta_i$, $S_{rz}=\sigma_r\cos\theta_r$, and $S_{tz}=\sigma_t\cos\theta_t$ for incident beam, reflected beam, and transmitted beam, respectively. The polarization degrees of the reflected and the transmitted beams are described by

$$\sigma_r=\frac{2f_pf_s|r_p||r_s|\sin[\psi-(\phi_p-\phi_s)]}{|r_p|^2f_p^2+|r_s|^2f_s^2}, \tag{32}$$

$$\sigma_t = \frac{2f_pf_s|t_p||t_s|\sin[\psi - (\varphi_p - \varphi_s)]}{|t_p|^2f_p^2 + |t_s|^2f_s^2}. \tag{33}$$

In the regime of partial reflection and transmission, the Fresnel coefficients are real ($\phi_A=0$ and $\varphi_A=0$). Hence, the polarization degree of the transmitted beam should be unreversed in the LHM. The physics underlying the unreversed spin-dependent transverse shifts is the unreversed spin angular momentum of photons. A further point that should be mentioned is that the unreversed angular momentum of photons can provide a physical explanation of our early prediction: the rotational Doppler effect in the LHM is unreversed, although the linear Doppler effect is reversed [38].

To obtain a clear physical picture of the spin Hall effect, we attempt to perform analyses on the z component of the total angular momentum for each of individual photons. The total angular-momentum law for single photon is given by [39]

$$-\Delta y_t k_t \sin\theta_t + \sigma_t \cos\theta_t = \sigma \cos\theta_i. \tag{34}$$

When the photon incident from air to a low-refractive-index medium, the incident angle is less than the refractive angle $\theta_i < |\theta_t|$. The linear polarized beam can be represented as a superposition of equal $\sigma=+1$ and $\sigma=-1$ photons. For the $\sigma=+1$ photons, the z component of spin angular momentum $\sigma_t \cos\theta_t(\sigma_t>0)$ decreases after entering the medium. Because of the conservation law, the total angular momentum must remain unchanged. To conserve the total angular momentum, the photon must move to the direction $-y(\Delta y_t<0)$ [Figs. 3(a) and 3(c)]. For the $\sigma=-1$ photons, the z component of spin angular momentum $\sigma_t \cos\theta_t(\sigma_t<0)$ increases. As a result, the photons must move to the direction $+y(\Delta y_t>0)$ [Figs. 3(b) and 3(d)]. When the beam incident from air to a high-refractive-index medium, the incident angle is less than the refractive angle $\theta_i > |\theta_t|$. The spin Hall effect exhibits a reversed version as shown in Fig. 4. This gives a simple way to understand how the light exhibits a spin Hall effect and why the spin Hall effect is unreversed in the LHM.

For the spin Hall effect of light, precise characterization requires measurement sensitivities at the angstrom level [10]. However, direct observation of the spin Hall effect is still remain an open challenge in condensed-matter physics [1–3] and high-energy physics [40,41]. Because of the close similarity in condensed-matter physics, high-energy physics, and optics, the spin Hall effect of light will provide indirect evidence in a diversity of physical systems [42]. In general, introducing the spin Hall effect into contemporary photonics and nano-optics may result in the development of a promising new area of research—spinoptics. Recently, the technique of transformation optics has emerged as a means of designing metamaterials that can bring about unprecedented control of electromagnetic fields [13]. It is possible that the paths of different circularly polarized components can be controlled by introducing a prescribed spatial variation in the constitutive parameters. Hence, the metamaterial is a good candidate to amplify the spin Hall effect.

IV. CONCLUSIONS

In conclusion, we have established a general propagation model to describe the spin Hall effect of light beam in the LHM. The spin-dependent transverse shift of beam centroid perpendicular to the refractive index gradient for the light beam through an air-LHM interface has been demonstrated. For a certain circularly polarized component, whether the transverse shift is positive or negative depends on the magnitude the refractive index gradient. We have revealed that the spin Hall effect in the LHM is unreversed, although the sign of refractive index gradient is reversed. The physics underlying the unreversed spin Hall effect is the unreversed spin angular momentum of photons. We have found that the angular shifts in the LHM possess a reversed version. The inherent secret of this intriguing effect is the negative diffraction. In the absence of loss, the angular shifts satisfy the total linear momentum conservation law and the transverse shifts fulfill the total angular-momentum conservation law. The study of the spin Hall effect will make a useful contribution to clarify the nature of photons in the LHM. Our results provide further evidence for that the linear momentum of photons is reversed, while the spin angular momentum is unreversed in the LHM.

ACKNOWLEDGMENTS

The authors are sincerely grateful to Professor A. Bérard for his helpful suggestions. This research was supported by the National Natural Science Foundation of China (Grant Nos. 10804029, 10974049, and 10904036).

[1] J. Sinova, D. Culcer, Q. Niu, N. A. Sinitsyn, T. Jungwirth, and A. H. MacDonald, Phys. Rev. Lett. **92**, 126603 (2004).

[2] S. Murakami, N. Nagaosa, and S. C. Zhang, Science **301**, 1348 (2003).

[3] J. Wunderlich, B. Kaestner, J. Sinova, and T. Jungwirth, Phys. Rev. Lett. **94**, 047204 (2005).

[4] M. Onoda, S. Murakami, and N. Nagaosa, Phys. Rev. Lett. **93**, 083901 (2004).

[5] K. Y. Bliokh and Y. P. Bliokh, Phys. Rev. Lett. **96**, 073903 (2006).

[6] O. Costa de Beauregard, Phys. Rev. **139**, B1443 (1965).

[7] F. Goos and H. Hänchen, Ann. Phys. **436**, 333 (1947).

[8] F. I. Fedorov, Dokl. Akad. Nauk SSSR **105**, 465 (1955).

[9] C. Imbert, Phys. Rev. D **5**, 787 (1972).

[10] O. Hosten and P. Kwiat, Science **319**, 787 (2008).

[11] R. A. Shelby, D. R. Smith, and S. Schultz, Science **292**, 77 (2001).

[12] V. G. Veselago, Sov. Phys. Usp. **10**, 509 (1968).

[13] J. Pendry, D. Schurig, and D. Smith, Science **312**, 1780 (2006).

[14] J. B. Pendry, Phys. Rev. Lett. **85**, 3966 (2000).

[15] Z. M. Zhang and C. J. Fu, Appl. Phys. Lett. **80**, 1097 (2002).

[16] P. R. Berman, Phys. Rev. E **66**, 067603 (2002).
[17] N. Seddon and T. Bearpark, Science **302**, 1537 (2003).
[18] J. Lu, T. M. Grzegorczyk, Y. Zhang, J. Pacheco, B. I. Wu, and J. A. Kong, Opt. Express **11**, 723 (2003).
[19] S. Riyopoulos, Opt. Lett. **31**, 2480 (2006).
[20] B. A. Kemp, J. A. Kong, and T. M. Grzegorczyk, Phys. Rev. A **75**, 053810 (2007).
[21] M. Scalora, G. D'Aguanno, N. Mattiucci, M. J. Bloemer, D. de Ceglia, M. Centini, A. Mandatori, C. Sibilia, N. Akozbek, M. G. Cappeddu, M. Fowler, and J. W. Haus, Opt. Express **15**, 508 (2007).
[22] V. Yannopapas and P. G. Galiatsatos, Phys. Rev. A **77**, 043819 (2008).
[23] R. A. Beth, Phys. Rev. **50**, 115 (1936).
[24] M. Lax, W. H. Louisell, and W. McKnight, Phys. Rev. A **11**, 1365 (1975).
[25] K. Y. Bliokh and Y. P. Bliokh, Phys. Rev. E **75**, 066609 (2007).
[26] A. Aiello and J. P. Woerdman, Opt. Lett. **33**, 1437 (2008).
[27] A. Aiello, M. Merano, and J. P. Woerdman, Opt. Lett. **34**, 1207 (2009).
[28] H. Luo, Z. Ren, W. Shu, and F. Li, Phys. Rev. E **75**, 026601 (2007).
[29] H. Luo, Z. Ren, W. Shu, and S. Wen, Phys. Rev. A **77**, 023812 (2008).
[30] C. Menzel, C. Rockstuhl, T. Paul, S. Fahr, and F. Lederer, Phys. Rev. A **77**, 013810 (2008).
[31] J. D. Jackson, *Classical Electrodynamics* (Wiley, New York, 1999).
[32] K. Y. Bliokh, I. V. Shadrivov, and Y. S. Kivshar, Opt. Lett. **34**, 389 (2009).
[33] C. Duval, Z. Horváth, and P. A. Horváthy, Phys. Rev. D **74**, 021701(R) (2006).
[34] C. M. Krowne, Phys. Lett. A **373**, 466 (2009).
[35] V. G. Fedoseyev, Opt. Commun. **282**, 1247 (2009).
[36] M. A. Player, J. Phys. A **20**, 3667 (1987).
[37] V. G. Fedoseyev, J. Phys. A **21**, 2045 (1988).
[38] H. Luo, S. Wen, W. Shu, Z. Tang, Y. Zou, and D. Fan, Phys. Rev. A **78**, 033805 (2008).
[39] M. Onoda, S. Murakami, and N. Nagaosa, Phys. Rev. E **74**, 066610 (2006).
[40] A. Bérard and H. Mohrbach, Phys. Lett. A **352**, 190 (2006).
[41] P. Gosselin, A. Bérard, and H. Mohrbach, Phys. Rev. D **75**, 084035 (2007).
[42] K. Y. Bliokh, A. Niv, V. Kleiner, and E. Hasman, Nature Photon. **2**, 748 (2008).